Distinct Nature of Static and Dynamic Magnetic Stripes in Cuprate Superconductors

H. Jacobsen, S. L. Holm, M.-E. Lăcătuşu, A. T. Rømer, M. Bertelsen, M. Boehm, R. Toft-Petersen, J.-C. Grivel, S. B. Emery, L. Udby, B. O. Wells, and K. Lefmann

Phys. Rev. Lett. **120**, 037003 — Published 18 January 2018

DOI: 10.1103/PhysRevLett.120.037003

On the distinct nature of static and dynamic magnetic stripes in cuprate superconductors

H. Jacobsen,[1,2] S. L. Holm,[1,3] M.-E. Lăcătuşu,[1,4] A. T. Rømer,[1] M. Bertelsen,[1] M. Boehm,[5] R. Toft-Petersen,[6,7] J.-C. Grivel,[4] S. B. Emery,[8,9] L. Udby,[1] B. O. Wells,[8] and K. Lefmann[1]

[1] *Nanoscience Center, Niels Bohr Institute, University of Copenhagen, 2100 Copenhagen Ø, Denmark*
[2] *Department of Physics, Oxford University, Oxford, OX1 3PU, United Kingdom*
[3] *Interdisciplinary Nanoscience Center - INANO-Kemi, 8000 Aarhus C, Denmark*
[4] *Institute of Energy Conversion, Technical University of Denmark, 4000 Roskilde, Denmark*
[5] *Institut Max Von Laue Paul Langevin, 38042 Grenoble, France*
[6] *Helmholtz-Zentrum Berlin, 14109 Berlin, Germany*
[7] *Department of Physics, Technical University of Denmark, 2800 Kgs. Lyngby, Denmark*
[8] *Department of Physics and Institute of Materials Science, University of Connecticut, Connecticut 06269, USA*
[9] *Present address: Naval Surface Warfare Center Indian Head EOD Technology Division, Indian Head, MD 20640 USA*

We present detailed neutron scattering studies of the static and dynamic stripes in an optimally doped high-temperature superconductor, La_2CuO_{4+y}. We observe that the dynamic stripes do not disperse towards the static stripes in the limit of vanishing energy transfer. Therefore, the dynamic stripes observed in neutron scattering experiments are not the Goldstone modes associated with the broken symmetry of the simultaneously observed static stripes, and the signals originate from different domains in the sample. These observations support real-space electronic phase separation in the crystal, where the static stripes in one phase are pinned versions of the dynamic stripes in the other, having slightly different periods. Our results explain earlier observations of unusual dispersions in underdoped $La_{2-x}Sr_xCuO_4$ ($x = 0.07$) and $La_{2-x}Ba_xCuO_4$ ($x = 0.095$).

An imperative open question in materials physics is the nature of high-temperature superconductivity. Unlike conventional superconductors, where the Cooper pairing mechanism is well-established [1], the pairing mechanism in high-temperature superconductors (HTS) still sparks controversy [2]. A comprehensive description of the electronic behavior inside HTS is indispensable to push this field of research onward. Hence, the magnetic structures which appear close to as well as inside the superconducting phase are still being studied intensively [3, 4]. In many HTS compounds, experiments indicate a modulated magnetic structure, consistent with superconducting "stripes" of charge separated by magnetic regions as sketched in Fig. 1a [5]. Magnetic excitations, referred to as "dynamic stripes", are found with similar periodicity, and are therefore thought to be related to the Goldstone modes of the static stripes [6].

Here we present evidence that this model is incomplete for a family of HTS. We find that the dynamic stripes do not disperse towards the static stripes in the limit of vanishing energy transfer and interpret this in terms of electronic phase separation, where static and dynamic stripes populate different spatial regions of the HTS.

Compounds based on the La_2CuO_4 family were the first high-temperature superconductors (HTS) to be discovered [7]. They become superconducting upon doping with electrons or holes, with a maximum critical temperature, $T_c \approx 40$ K, whether the dopant is Sr ($La_{2-x}Sr_xCuO_4$, LSCO), Ba ($La_{2-x}Ba_xCuO_4$, LBCO), or O (La_2CuO_{4+y}, LCO+O). The generic crystal structure of these compounds is illustrated in Fig. 1b. They consist of planes of CuO separated by layers of La/Sr/Ba. Each Cu atom is at the center of an octahedron of oxygen atoms. At elevated temperatures these materials are in the high-temperature tetragonal (HTT) phase. Upon lowering the temperature, the crystals enter the low-temperature orthorhombic phase (LTO) where the oxygen octahedra tilt around the tetragonal a axes, leading to a change in lattice parameters, $a < b$ and to possible twinning [9, 10], see Supplementary Material for details [8].

Since the first discovery, a multitude of HTS have been found in the cuprate family. The amplitude and period of the stripe order modulations vary strongly with the choice and amount of dopant, with static stripes being particularly pronounced in LCO+O [11].

The spin stripes can be measured using magnetic neutron scattering, where they are observed as pairs of intensity peaks at incommensurate (IC) wave vector transfers, e.g. at $\mathbf{Q} = (1 + \delta_h, \delta_k, 0)$ and $\mathbf{Q} = (1 - \delta_h, -\delta_k, 0)$ for stripes along the (110) direction, see Fig. 1c. Here, the components of the scattering vector are given in terms of $(2\pi/a, 2\pi/b, 2\pi/c)$, where a, b and c are the orthorhombic lattice constants. The real-space modulation period is $L \sim (2\pi/\delta)a$, and we refer to δ as the incommensurability of the stripes. Typically $\delta_h \approx \delta_k$, indicating that the modulation is approximately along the Cu-O-Cu bonds (the (110) and $(1\bar{1}0)$ directions), although variations have been reported, indicating a kink in the stripes after a number of unit cells [11, 12].

Typically, stripes are observed not only at the above mentioned positions, but also at $\mathbf{Q} = (1 - \delta_h, \delta_k, 0)$ and

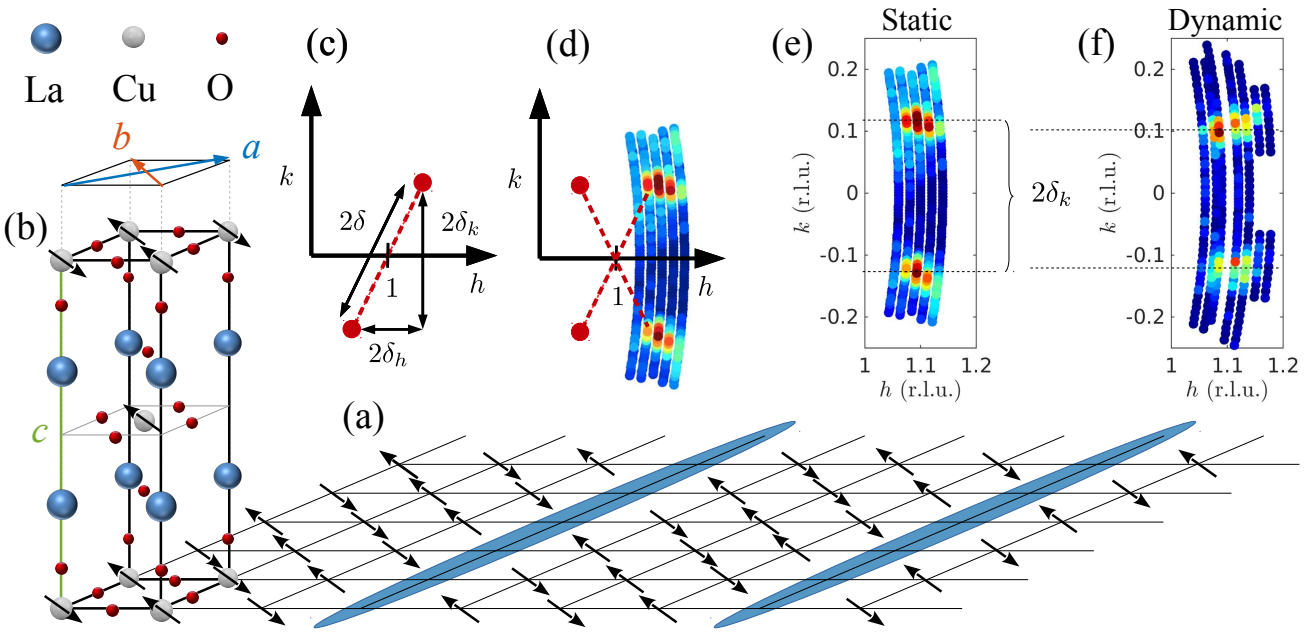

Figure 1. Sketch of magnetic and charge stripes in the cuprate high-temperature superconductor $La_2CuO_{4+\delta}$ (LCO+O). (a) Illustration of magnetic stripes with a period of 8, concurrent with period 4 charge stripes along the Cu-O-Cu bond directions (broad blue lines). Another type of domains exists, where the stripes are rotated 90 degrees, still lying within the plane (not shown). (b) The tetragonal unit cell of LCO+O illustrating the spins on the Cu ions. The spins are aligned along the orthorhombic b-axis, shown above the unit cell. (c) Illustration of reciprocal space (in orthorhombic notation) showing the position of the incommensurate magnetic stripe peaks for stripes approximately along the (110) direction. The difference between δ_h and δ_k is exaggerated for clarity. (d) the quartet of peaks around the (100) position observed when stripes are present along both the (110) and (1$\bar{1}$0) directions. The coloured regions show the regions probed in the present experiment. (e) Example of the static ($\Delta E = 0$) and (f) dynamic ($\Delta E = 1.5$ meV) stripe signal in LCO+O, measured by neutron scattering.

$\mathbf{Q} = (1 + \delta_h, -\delta_k, 0)$, giving rise to a quartet of peaks around the (100) position, as illustrated in Fig. 1d. This indicates that the compound exhibits stripes (approximately) along both the (110) and (1$\bar{1}$0) directions, most likely by the stripes in adjacent layers alternating between the (110) and (1$\bar{1}$0) directions [13].

Inelastic neutron scattering has shown the presence of dynamic stripes, which at low energies have similar modulation period as the static stripes [14]. The modulation period of the stripes is found to be almost constant up to energy transfers of $\Delta E \sim 10 - 15$ meV [15, 16]. In the cuprates an hourglass shaped dispersion develops at higher energies [17].

The incommensurability of the stripes varies with doping. In the LSCO-type cuprates, δ increases linearly with doping and saturates at a maximal value of $\delta = 1/8$ [14]. In some cuprates, similar stripes of charge with half the modulation period have been observed using X-ray diffraction, validating the picture of magnetic and charge stripes in Fig. 1a [18–22]. However, the energy resolution of X-rays does not allow to distinguish between static and dynamic stripes.

We have used elastic and inelastic scattering of low energy neutrons to accurately measure the reciprocal space position of the static and dynamic stripes in highly oxygenated LCO+O in the LTO phase. The experiments were performed at the cold-neutron triple axis spectrometers FLEXX at HZB, Berlin [24], and ThALES at ILL, Grenoble [25]. The elastic energy resolution in the ThALES experiment was 0.24 meV (Full Width at Half Max, FWHM), while the Q resolution was 0.05 r.l.u. (FWHM). For further details on the experiments, see the Supplementary Material [8].

Panel (d) of Fig. 1 shows how we probe two of the four IC peaks in our neutron scattering experiments. The actual data for a series of scans are shown in panels (e) and (f) as 2D colorplots. Fig. 2 shows examples of the scans through the center of the peaks at 0 and 1.5 meV energy transfer, probing the static and dynamic stripes, respectively. The inset illustrates the direction of the scans in reciprocal space.

To eliminate errors from minor misalignments, we determine the incommensurability along k, δ_k, as half the distance between the peak centers. In Fig. 3 we display δ_k for all energy transfers probed in the experiment at two temperatures. As expected, the dynamic stripes appear at the same reciprocal space position in the normal phase (45 K) as in the SC phase (2 K) (within the instrument resolution), whereas the static stripes are only present at low temperature. The elastic stripes are found to be ro-

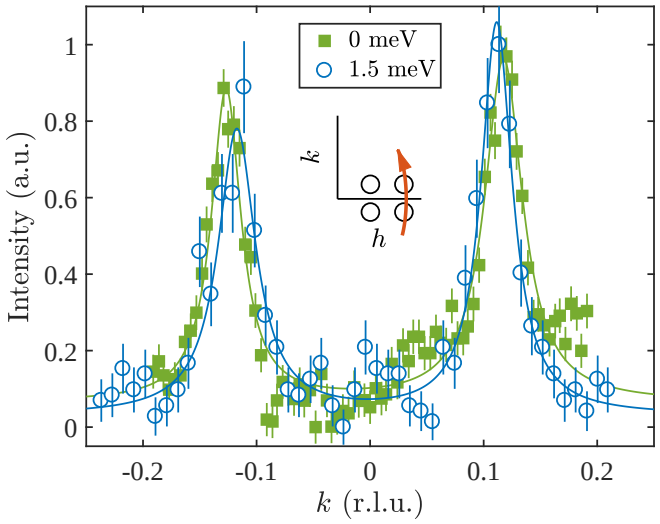

Figure 2. Neutron scattering data for LCO+O scanned along the direction shown in the insets, showing the shift in peak position between the elastic stripes (green) and low-energy inelastic stripes (blue). The data have been rescaled and the background subtracted.

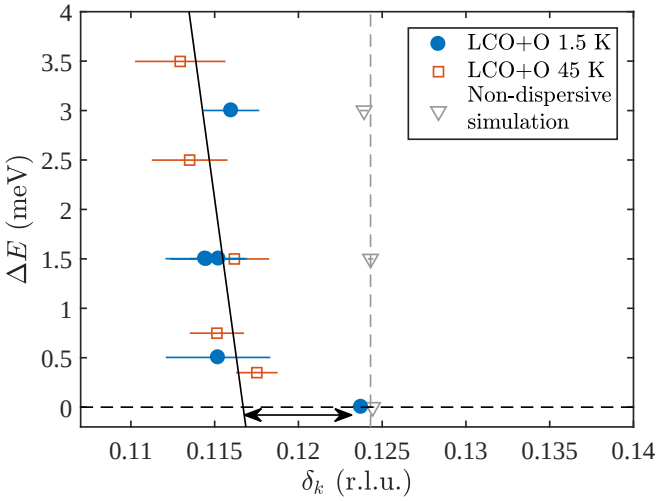

Figure 3. The incommensurability, δ_k at different energy transfers ΔE for LCO+O. A significant shift is seen between the elastic and inelastic data. The solid black line is a linear fit to the dispersion for $\Delta E > 0$. Gray triangles represent the dispersion relation obtained from simulated data, where the simulated dispersion relation is vertical.

tated by 7° from the Cu-O-Cu bond directions, while the observed inelastic stripes are rotated by 3°. The inelastic dispersion appears continuous and steep, consistent with earlier cuprate results [15, 16]. However, the elastic signal shows a large and significant difference in δ_k, appearing as a discontinuity in the dispersion relation at vanishing energy transfer. Similar observations have been briefly remarked upon in underdoped $La_{2-x}Sr_xCuO_4$ ($x = 0.07$) [26] and $La_{2-x}Ba_xCuO_4$ ($x = 0.095$) [27]. In both cases the observation was left unexplained.

To rule out that these surprising differences in δ_k and the stripe rotation are artifacts caused by experimental non-idealities, we have performed a virtual ray-tracing experiment in McStas [28, 29]. The simulations use a precise model of the experiment including the guide system [30], monochromator, sample, analyzer and detector; details can be found in the Supplementary Material [8]. This method is known to accurately reproduce experimental effects like peak broadening and displacement [31]. The virtual experiments exclude misalignment of the instrument as a cause of the effect and show that the experimental resolution can cause a tiny shift in the observed incommensurability, see Fig. 3.

The experimentally observed shift in peak position is, however, more than an order of magnitude larger than what can be explained by instrument effects, and is therefore a genuine property of the sample. Hence, in order not to violate the Goldstone's theorem, the static and dynamic stripes must originate from different regions in the sample. There are two probable ways this can occur:

First, the dynamic stripes could be transverse fluctuations from the static stripe order, resembling ordinary spin waves. Due to the neutron scattering selection rules, the scattering observed in the elastic and inelastic channels stem from different twin domains as explained in detail in the Supplementary Material [8]. This results in a shift in the observed peak position between the elastic and inelastic channels, comparable to the observed shift. The magnitude and direction of the shift due to twinning depends heavily on δ_h and δ_k and requires $\delta_h < \delta_k$. Secondly, the static and dynamic spin response may originate from different microscopic regions which are not related by twinning. This suggests a real-space electronic phase separation of the crystal into regions with two different spin structures; one domain type which has static stripe order and associated dynamic stripes, and another type of domain where only dynamic stripes are present.

At first glance the twinning model seems to provide an explanation of our data. However, it fails to explain the similar observations in LBCO (where $\delta_h = \delta_k$) mentioned above [27], as the model requires $\delta_h < \delta_k$. Furthermore, the model relies on the assumption that the four twin domains display only one type of stripe order with associated transverse excitations. Most likely these assumptions are too simplified and relaxing any of them reduces the effect of twinning on the observed signal. We therefore turn to the second model: electronic phase separation.

Muon spin rotation experiments on highly oxygenated LCO+O show that the material electronically phase separates into a magnetic (A) and a superconducting (B) phase of roughly equal volume [32, 33] and transition temperature $T_c \approx T_N \sim 40$ K with the present slow cooling conditions. Based on these experiments we propose

the following properties of the two phases:

Phase A is underdoped (resembling LSCO with $n_h = 0.125$) and has static magnetism (and weak fluctuations), responsible for the observed static signal and a small fraction of the dynamic signal. Phase B is optimally doped (resembling LSCO with $n_h = 0.16$) and superconducting with strong fluctuations, responsible for (the majority of) the observed dynamic signal.

We note that no spin gap was observed below T_c in our experiments. Absence of a spin gap was also observed in the experiments on strongly underdoped LSCO [26] and LBCO [27], mentioned above. Both materials were suggested not to be d-wave superconductors but instead display Pair Density Wave (PDW) superconductivity [4, 34]. Our results are consistent with this interpretation. A PDW state would require some degree of magnetic order in the SC phase, but this may be extremely weak and thus effectively invisible in our experiments. The simultaneous observation of gapless excitations and a shift in incommensurability in all three compounds suggests a connection between the two effects. The gapless excitations are likely a result of a PDW state in the sample, while the shift is caused by electronic phase separation. At present it is unclear whether these two behaviours are related.

The critical temperature of the superconducting phase, T_c, coincides with the Néel temperature of the magnetic phase, T_N, such that above this temperature superconductivity and the static magnetism disappear, but strong stripe fluctuations remain. The fact that $T_c \approx T_N$ is likely not coincidental, but it is unclear whether the electronic phase separation is caused by, or is the cause of, the close proximity of T_c and T_N. We suggest a scenario where the ground state energy for phase A and phase B are very close and lowering the temperature below T_c will cause an electronic phase separation with concurrent static magnetism and superconductivity. The spatial distribution of impurity potentials as well as inhomogeneous hole doping becomes important parameters that can tip a region towards becoming type A or B, e.g. by pinning.

The relative population of each phase is primarily controlled by the total number of holes, but can also be influenced by an applied magnetic field or by crash cooling [11, 35]. In the case of LCO+O, crash cooling can further inflict a lowering of T_c which has been explained by disconnection of the optimally superconducting pathways [36].

The crucial point is that although the two phases are closely related, there is no a priori reason why the stripe order in phase A and the stripe dynamics in phase B should have the same incommensurability. Indeed, our results show that this is not the case. This indicates that other properties of the stripes may not be identical either, and one should thus be extremely careful when interpreting neutron scattering data on stripes.

Phase separation has been suggested to occur in a number of cuprates or related compounds, a few of which we will mention here. LSCO with $x = 0.12$ has been suggested to phase separate into microscopic superconducting regions with gapped dynamic stripes and non-superconducting regions with static stripes [37]. Spontaneous, microscopic phase separation has also been observed in purely oxygen doped LCO+O crystals [33] and in crystals doped with both oxygen and strontium [38]. Furthermore, recent studies of $La_{5/3}Sr_{1/3}CoO_4$ show evidence of microscopic phase separation into components with different local hole concentration [39, 40]. In the latter material the upper and lower parts of the hourglass dispersion are even proposed to originate from different nano-scale structures in the sample [39]. No discrepancy in the incommensurability between static and dynamic stripes was reported in these studies.

The idea of dynamic and static stripes having different origin is supported by a number of other observations. For example, the static and dynamic stripes exhibit different behaviors as function of temperature. In underdoped LSCO and in LCO+O as evidenced in this experiment, the static stripes vanish above T_c, but the dynamic stripes remain to far higher temperatures [41–43]. In contrast, in the optimally doped region, the static stripes are altogether absent, while the dynamic stribe exist above a certain energy gap [16]. In the heavily overdoped region it has been shown that substituting small amounts of Fe for Cu induces static magnetism [44]. The incommensurability of the induced magnetic order is governed by nesting of the underlying Fermi surface and differs from the 1/8 periodicity of the low-energy dynamic stripes.

When applying a magnetic field, the static stripes are in general strengthened [41, 42, 45–48], with a few exceptions [47, 49]. In many cases this happens with an accompanying change in the dynamic stripe spectrum [41, 42, 45], but in other cases, the dynamic stripe spectrum is unchanged [46]. Hence, the coupling between static and dynamic stripes is not simple and unique.

In conclusion we have found that the dynamic stripes do not disperse towards the static stripes in the limit of vanishing energy transfer in a HTSC. The effect is subtle and requires high flux and good resolution such as provided by the ThALES spectrometer in order to be observed. Our findings are, however, of prime importance, since they suggest that the observed static and dynamic stripes originate from different electronic phases in the sample, where one of these phases is likely to be a competitor for superconductivity with the development of static stripe order.

Our observations are relevant for all compounds displaying stripe order. As an example, the structurally similar, but non-superconducting compound $(La,Sr)_2NiO_4$ (LSNO) displays magnetic and charge stripes with the dynamic stripes persisting at higher temperatures than the ordering temperature [50]. In some of these compounds it has also been observed that the ordering vec-

tor of the static and dynamic stripes do not coincide at vanishing energy transfer [51]. We speculate that a similar electronic phase separation could be in play here, as we suggest for LCO+O. It is likely that this mechanism also explains earlier observations of unusual dispersions in LSCO [26] and LBCO [27]. Our findings may thus be a vital part in unveiling the nature of high temperature superconductivity.

We thank ILL, Grenoble, France, and HZB, Berlin, Germany for providing us access to their neutron scattering facilities. We are indebted to E. Farhi for providing us with a model of the ILL neutron guide system for use in the Monte Carlo simulations. We thank N. B. Christensen, P. J. Ray, J. M. Tranquada, J.I. Budnick, P.G. Freeman, M. Skoulatos, and D. Prabhakaran for illuminating discussions. We thank P. J. Ray for help with some of the figures.

Work at University of Connecticut was supported by the USDOE Basic Energy Sciences under contract DE-FG02-00ER45801. The work was supported by the Danish Research Council FNU through the grants DanScatt and Magnetism in Superconductors.

[1] J. Bardeen, L.N. Cooper and J.R. Schrieffer, Phys. Rev. **108**, 1175 (1957).
[2] A. J. Leggett, Nature Physics **2**, 134 (2006).
[3] B. Keimer *et al.*, Nature **518**, 179 (2015).
[4] E. Fradkin, S. Kivelson and J. M. Tranquada, Rev. Mod. Phys. **87**, 457 (2015).
[5] J. M. Tranquada *et al.*, Nature **375**, 561 (1995).
[6] M. Vojta, Adv. Phys. **58**, 699 (2009); and references therein.
[7] J. G. Bednorz and K. A. Müller, Z. Phys. B **64**, 189 (1986).
[8] See Supplementary Material for details.
[9] M. Braden *et al.*, Physica C **191**, 455 (1992).
[10] P. J. Ray, M. Sc. thesis, University of Copenhagen (2015).
[11] Y. S. Lee *et al.*, Phys. Rev. B **60**, 3643 (1999).
[12] H. Kimura *et al.*, Phys. Rev. B **61**, 14366 (2000).
[13] M. Hücker *et al.*, Phys. Rev. B **83**, 104506 (2011).
[14] K. Yamada *et al.*, Phys. Rev. B **57**, 6165 (1998).
[15] N. B. Christensen *et al.*, Phys. Rev. B **83**, 104506 (2011).
[16] B. Lake *et al.*, Nature **400**, 43 (2002).
[17] B. Vignolle *et al.*, Nature Physics **3**, 163 (2007).
[18] J. Chang *et al.*, Nature Physics **8**, 871 (2012)
[19] E. H. da Silva Neto *et al.*, Science **343**, 393 (2014).
[20] V. Thampy *et al.*, Phys. Rev. B **90**, 100510 (2014).
[21] T. P. Croft *et al.*, Phys. Rev. B **89**, 224513 (2014).
[22] X. M. Chen *et al.*, Phys. Rev. Lett. **117**, 167001 (2016)
[23] H. Woo *et al.*, Phys. Rev. B **72**, 064437 (2005).
[24] M.D. Le *et al.*, Nucl. Instr. Meth. A **729**, 220 (2013).
[25] K. Lefmann *et al.*, Institut Laue-Langevin data set, doi:10.5291/ILL-DATA.TEST-2473.
[26] H. Jacobsen *et al.*, Phys. Rev. B **92**, 174525 (2015).
[27] Z. Xu *et al.*, Phys. Rev. Lett. **113**, 177002 (2014).
[28] K. Lefmann and K. Nielsen Neutron News **10,** 20, (1999).
[29] P. Willendrup, E. Farhi and K. Lefmann Physica B, **350,** e735 (2004).
[30] E. Farhi, personal communication (2015).
[31] L. Udby *et al.*, Nucl. Instr. Meth. A **634**, S138 (2011).
[32] A. T. Savici *et al.*, Phys. Rev. B , **66**, 014524 (2002)
[33] H. E. Mohottala *et al.*, Nature Materials **5**, 377 (2006).
[34] M. H. Christensen, H. Jacobsen, T. A. Maier, and B. M. Andersen, Phys. Rev. Lett., **116**, 167001 (2016).
[35] A.T. Rømer *et al.*, Phys. Rev. B **91**, 174507 (2015).
[36] M. Fratini *et al.*, Nature **466** 841 (2010)
[37] M. Kofu *et al.*, Phys. Rev. Lett. **102**, 047001 (2009).
[38] L. Udby *et al.*, Phys. Rev. Lett. **111**, 227001 (2013).
[39] Y. Drees *et al.*, Nature Comm. **5**, 5731 (2014).
[40] P. Babkevich *et al.*, Nature Comm. **7**, 11632 (2016).
[41] B. Lake *et al.*, Nature **415**, 299 (2002).
[42] B. Lake *et al.*, Science **291**, 1759 (2001).
[43] C. Lee *et al.*, J. Phys. Soc. Jpn. **69**, 1170-1176 (2000).
[44] R.-H. He *et al.*, Phys. Rev. Lett. **107**, 127002 (2011).
[45] J. Chang *et al.*, Phys. Rev. Lett. **102**, 177006 (2009).
[46] A. T. Rømer *et al.*, Phys. Rev. B **87**, 144513 (2013).
[47] J. Chang *et al.*, Phys. Rev. B **78**, 104525 (2008).
[48] Y. S. Lee *et al.*, Phys. Rev B **69** 020502R (2004)
[49] L. Udby *et al.*, Phys. Rev. B **80**, 014505 (2009).
[50] S. Anissimova *et al*, Nature Comm. **5**, 3467 (2014).
[51] Paul Freeman (personal communication, 2017).